

MIXED CONVECTION BETWEEN HORIZONTAL PARALLEL PLATES

دراسة المصل المختلط بين لوهين متساوين متوازيين

M. S. YASEL, M. MAHGOUB, M. S. GHITH

Mechanical Power Eng., Faculty of Engineering,
Mansoura University, Mansoura, Egypt

خلاصة :

في هذا البحث تم دراسة السريان الرقائقي مع وجود حمل مختلط في منطقة المدخل بين لوهين متساوين متوازيين ، ذي درجة حرارة ثابتة . ولضمان تحالف السريان حول محورة [فترص] تسخين المائع من اللوح السفلي في حين برد من اللوح العلوي . للتعامل مع معادلات الحركة في الإتجاه الطولى والعمودى عليه ، ومعادلة الطاقة الواصلة للسريان فقد تم تعريف المتغيرات المستقلة والتابعة في صورة لا بعديه مناسبة يمكن معالتها بطريقة المل الشابهين المثلث . وقد تم حل المعادلات المعدلة مذكورة بطريقة رونج - كوتا متوجة بطريقة الرسم لتحقق الشرط المدية للمسألة . وامكن الحصول على نتائج لكل من توزيعات السرعة ودرجة الحرارة عند قطاعات مختلفة ، وكذلك معامل الإحتكاك ورقم نوسلت بطول الممر وذلك لقيم براندتل تتراوح بين ٠، الى ٢ ومن المدى ٣٠٠ الى ٤٠ ، لمعامل المصل . كما تم بحث تأثير المسافة بين اللوهين بتغيير معامل الشكل بين ٠، الى ٧٥ - ١٠ - ١٥ . تبين من النتائج حدوث زيادة في رقم نوسلت المصل ومعامل الإحتكاك المثلث عند زيادة معامل المصل او إسقاطه معامل الشكل . كما لوحظ زيادة معامل [نفع] الحرارة بزيادة رقم براندتل .

Abstract

Laminar mixed convection flow in the entrance region between two horizontal parallel plates isothermally heated from below and cooled from above is studied numerically by the local similarity solution method . According to this method the proper dimensionless forms of the momentum and energy equations are transformed to a simpler system of ordinary differential equations which are solved numerically by the Runge-Kutta integration technique along with Newton-Raphson shooting method for the boundary value problems . Accordingly the coefficient of friction , local heat transfer and velocity and temperature distributions are computed for fluids having Prandtl numbers of 0.5, 0.7, 1.0 and 2.0 for values of the defined buoyancy parameter ranging from 0.033 to 0.2 while the height parameter values are taken as 0.5, 0.75 and 1. Numerical results reveal that the increase of the buoyancy parameter results in an increase in Nusselt number and enhances the heat transfer process and the higher values of Prandtl number lead to higher values of Nusselt number . Velocity and temperature profiles show remarkable difference from those of the pure forced convection .

NOMENCLATURE

- δ : The vertical distance from the lower plate to the axis of symmetry .
 β : The dimensionless coefficient of buoyancy . $\beta = \frac{g\alpha}{kT_0}$

ϕ	the dimensionless stream function, $\sqrt{u_0} \psi / \lambda$
g	gravitational acceleration
Gr_x	Grashof number defined as, $g\beta CT_w - T_0 \alpha^3 \lambda^2$
Gr_z	Grashof number defined as, $g\beta CT_w - T_0 \alpha^3 \lambda^2$
h	local heat transfer coefficient
k	coefficient of thermal conductivity
Nu_b	local Nusselt number defined as, $h\lambda/k$
Nu	local Nusselt number based on x , $h\lambda/k$
P	pressure
Pr	Prandtl number, ν/κ
q_w	heat flux at the wall
Re_b	Reynolds number defined as, $u_0 b / \nu$
Re_x	Reynolds number defined as, $u_0 x / \nu$
T	temperature
T_0	fluid temperature at the axis of symmetry
T_w	temperature of the plate
u	velocity component in the x direction
U_∞	free stream velocity
v	velocity component in the y direction
x	co-ordinate in the longitudinal direction
y	co-ordinate normal to the longitudinal direction
β	coefficient of thermal diffusivity
γ	coefficient of thermal expansion
η	dimensionless independent variable, $y\sqrt{u_0/\lambda}$
η_{axis}	the value of the independent variable η at the axis of symmetry (i.e. at $x=b/2$)
ζ	Bouyancy parameter, $Gr_x / Re_x^{5/2}$
ζ_0	height parameter, Gr_z / Re_z^2
ν	kinematic viscosity
ρ	density
ϑ	dimensionless temperature, $(T-T_0)/(CT_w - T_0)$
τ_w	wall shear stress, $\mu_p \frac{\partial u}{\partial y} \Big _w$
ψ	stream function, $\sqrt{u_0} \psi$

1. INTRODUCTION

In laminar forced convection flow, the effect of buoyancy forces becomes increasingly important as the flow velocity decreases and the temperature difference between the surface and the free stream increases. When heat is transferred between the walls and the adjacent fluid, the density of the fluid near the wall decreases and the buoy-

forced convection due to this density change cause the hotter fluid to move upward to the center and the cooler fluid at the center to move downward to the lower plate, thus a circulatory motion is superimposed on the main flow. This secondary motion induces either an aiding or an opposing pressure gradient which modifies the hydrodynamic and thermal fields and enhances the heat transfer rate between the walls and the free stream. In recent years attention has been focused on this problem. Sparrow and Minkowycz [1] investigated the conditions under which there are significant effects of buoyancy on a forced convection boundary layer flow over a flat plate using a perturbation series in terms of the buoyancy parameter. Osborne and Incropera [2] performed an experimental study for laminar water flow in the thermal entrance region of a horizontal duct and obtained correlation for Nusselt number in terms of the inverse Rayleigh number. Schneider [3] obtained an exact similarity solution for laminar flow over a flat plate heated from below in case of a wall temperature that is inversely proportional to the square root of the distance from the leading edge. His solution is limited to large values of the buoyancy parameter. Theoretical [4] and experimental [5] work by Kennedy and Leob studied the effect of buoyancy forces, from local heat sources, on laminar forced convection between parallel horizontal plates. Excellent agreement between the two studies is evidenced for small values of the buoyancy parameter equal to 0.16 up to 1.126. An increase in the heat flux created greater discrepancies in the results. Abu-Ellail and Marcos [6] implemented a numerical method to study the buoyancy effects in the entrance region for water flow in horizontal rectangular channels having aspect ratios of 1 and 4 for values of Froude number ranging from 1 to 20. The method was a combined iterative-marching integration technique to solve the finite difference governing equations. Heat transfer results showed that Nusselt Number deviates from the case of forced convection at certain axial distance depending on the value of Rayleigh number. The effect of increasing Rayleigh number was found to decrease the entry length. Numerical instability was encountered at $Re = 10^4$. Cheng and Hwang [7] developed a numerical solution for steady fully developed laminar forced convection with secondary flow caused by buoyancy forces in horizontal rectangular channels having aspect ratios ranging from 0.2 to 5 by the successive over-relaxation method. In this study the axial temperature was taken to be linear and the range of the parameter $Re \cdot Ra$ varied from 3000^3 to 3000^5 , the method diverges for higher values. A theoretical study by Wu, Cheng and Lin [8] handled the problem of fully developed laminar convection with upward flow in inclined rectangular channels under the thermal boundary conditions of axially uniform wall heat flux or constant wall temperature gradient for Froude number of 1 and 4, aspect ratios of 1.5 and 1. The inclination angle effect was presented in the study. Chen, Sparrow and Yu [9, 10, 11] obtained numerical results for the laminar heat

transfer and shear stress for laminar flow within the horizontal flat plate by the local similarity and local non-similarity methods for gases having Prandtl number of 0.7 and for values of the buoyancy parameter from 0.03 to 1. Supplément buoyancy effects were found for 0.03 Grav-Ray=0.03.

The present paper describes a numerical study on laminar combined free and forced convection flow and heat transfer in the entrance region between two horizontal parallel plates heated from below and cooled from above. In such case the induced buoyancy forces at both the lower and upper plates produce an accelerating pressure gradient along the main flow direction, then if the temperature difference between the lower plate and the free stream is assumed equal to that between the free stream and the upper plate; the flow will be symmetrical about the axis of the passage. This problem is of particular interest for flows through parallel plate passages in chemical vapour deposition, food processing industries, design of heat exchangers, cooling of nuclear reactors and cooling of the electronic circuitry.

2. GOVERNING EQUATIONS

Consideration is given to steady laminar convection flow in the entrance region between two horizontal parallel plates heated from below and cooled from above as shown in figure (1). The theoretical analysis is based on Boussinesq approximation, i.e., the physical properties of the fluid are assumed to be constant except for the density ρ in the buoyancy term.

The governing equations describing the considered flow are:

$$\frac{\partial u}{\partial x} = \frac{\partial v}{\partial y} = 0 \quad (1)$$

$$u \frac{\partial u}{\partial x} + v \frac{\partial u}{\partial y} = - \frac{1}{\rho} \frac{\partial p}{\partial x} + v \frac{\partial^2 u}{\partial y^2} \quad (2)$$

$$\frac{1}{\rho} \frac{\partial p}{\partial y} = g\beta C(T-T_0) \quad (3)$$

$$u \frac{\partial T}{\partial x} + v \frac{\partial T}{\partial y} = v \frac{\partial^2 T}{\partial y^2} \quad (4)$$

The system of equations(1-4) has to satisfy the following boundary conditions:

$$u=0, \quad T=T_0 \quad \text{at } y=0,$$

$$u=u_0, \quad T=T_0 \quad \text{at } y=b/2, \quad (45)$$

where u, v are the velocity components in x, y directions respectively. T denotes the temperature at general position x, y .

Because of the symmetry of flow about the axis of the passage only the lower half of the passage will be considered in this analysis.

To eliminate the pressure gradient from the governing equations (2-3), these equations are differentiated with respect to y, x respectively and by subtraction, the two momentum equations are transformed to one momentum equation.

To express the governing equations in a dimensionless form, new independent variables ξ, η along with a dimensionless temperature θ and a dimensionless stream function f are introduced according to the following definitions:

$$\xi = Gr_x / Rex^{5/2}, \quad \eta = y \sqrt{u_0 / \nu x}, \quad (46)$$

$$\theta = \frac{(T - T_0)}{(Tw - T_0)}, \quad (47)$$

$$f(\xi, \eta) = \psi \times \sqrt{u_0 \nu x} \quad (48)$$

where Gr_x is the local Grashof number defined as $g\beta(T_w - T_0) x^3 / \nu^2$, Rex is the local Reynolds number, defined as $u_0 x / \nu$. w is the stream function defined such that it satisfies the continuity equation (1).

Substituting the above defined dimensionless variables in the momentum and energy equations, these equations could be transformed to a dimensionless form as follows;

$$2f''' + f' f'' + f f''' + \xi \eta \theta' \\ = \xi \left(f \frac{\partial f''}{\partial \xi} + f' \frac{\partial f}{\partial \xi} + \xi \frac{\partial \theta}{\partial \xi} \right), \quad (49)$$

$$(2/\Pr) \theta' + \eta \theta'' = f' \frac{\partial \theta}{\partial \xi} - \theta \frac{\partial f}{\partial \xi} > 0, \quad (50)$$

with the boundary conditions;

$$f(\xi=0) = f'(\xi=0) = 0, \quad \theta(\xi=0) = 1,$$

$$\theta'(\xi_{max}) = \eta f'(\xi_{max}) = \theta(\xi_{max}) = 0, \quad (51)$$

where primes denote partial differentiation with respect to ξ .

The dimensionless variable η shown in the boundary conditions is the value of ξ corresponding to $x=0$ which is obtained from equation (6) as:

$$\eta_{\max} = \frac{1}{2} \sqrt{\frac{U_0}{\nu}} \xi_{\max} \quad (130)$$

After some manipulations equation (120) can be rewritten as follows,

$$\eta_{\max} = \zeta_b \cdot f \quad (130)$$

where :

$$\zeta_b = \frac{2}{3} \frac{\nu}{U_0} \cdot \text{Re}_b^2 = \frac{C_0 \rho C T_0 - T_0}{U_0^2} \cdot \frac{U_0^2}{\nu} \cdot b$$

The new independent variable ζ_b in equation (130) is directly proportional to the distance between the two plates and it will be dealt with as a parameter of the problem.

From the point of view of the local similarity method the terms containing partial derivatives with respect to ξ are considered sufficiently small and can be dropped from the momentum and energy equations. Integrating the obtained momentum equation with respect to η , one obtains the final form of the governing equations as follows:

$$f + \frac{d}{dx}(ff') - \left(\nu \frac{d^2 f}{dx^2} + \int f d\eta \right) = 0 \quad (14)$$

$$(2 + Pr) \theta' + f \theta = 0 \quad (15)$$

with the boundary conditions

$$f = f' = 0, \quad \nu = 1 \quad \text{at } \eta = 0$$

$$f' = \theta = \theta' = 0 \quad \text{at } \eta = \eta_{\max} \quad (16)$$

Equations (14)-(15) subject to the boundary conditions (16), are coupled ordinary differential equations and must be solved simultaneously.

Obtaining the velocity and temperature fields the local Nusselt number (Nu or Nu_b) and the local coefficient of friction (C_f defined as:

$$Nu = h b / \kappa, \quad Nu_b = h b / k \quad \text{and} \quad C_f = \tau_w / \rho U_0^2 \quad (17)$$

$$\text{where } \tau_w = \rho U_0 \left(\frac{\partial u}{\partial y} \right)_{y=0} \cdot$$

$$u = \zeta_b \cdot (C_0 - T_0) \cdot \frac{1}{2} - \frac{\partial u}{\partial y} \Big|_{y=0} \cdot (C_0 - T_0) \quad (18)$$

can be expressed after relating them to θ and f' at the wall in the following manner:

$$\text{Nu}_x \sqrt{\text{Re}_x} = 90f'_w(0).$$

$$\text{Nu}_b = 2\theta_{max} \cdot g(\xi_b, 0).$$

$$C_1 \sqrt{\text{Re}_x} = f''(\xi_b, 0).$$

3. NUMERICAL PROCEDURE

The numerical technique used to treat the governing equations (14-15) with their boundary conditions (16) entails transforming these equations to a set of five first order differential equations such that the Runge-Kutta integration technique can be employed to solve these equations with the boundary conditions (16) for a certain passage height (C or a certain ξ_b) over the whole range of the buoyancy parameter ξ . Then the process is repeated for different values of ξ_b or for different passage heights.

To start the solution, initial assumptions for f'' , θ' at the wall as well as f' at the axis of symmetry are employed to solve the momentum and energy equations simultaneously. Here the computed terminal values of f' , $f'_w(0)$ and θ' at the axis are functions of the initial assumptions and the correct values of f' and θ' at the wall are obtained by employing the iterative Newton-Raphson shooting method for the boundary value problems to satisfy the boundary values of $f''(0)$, $\theta'(0)$ at the axis and the assumed value of f'' as well, then the correct value of f' at the axis can be obtained by adjusting the produced velocity profile to satisfy the continuity equation in the integral form;

$$\theta_{max} = \int_0^{R_{max}} f' dx$$

This requires an additional shooting to obtain improved values for f' at the axis which is used to replace the initial assumption and an improved solution may then be computed. This was repeated few times leading to successive improvements until the tolerances preassigned to the values of f' , θ' , θ at the axis are achieved while the velocity profile satisfies the continuity equation to within a prescribed tolerance. A grid of 200 points was found quite sufficient, and the tolerances preassigned to $f''(0)$ and θ' at

the axis and for $\int f' dx$ were $8 \times 10^{-4}, 10^{-5}$ and 10^{-8} respectively.

4. RESULTS AND DISCUSSION

Numerical calculations are carried out for Prandtl number values of 0.5, 0.7, 1 and 2 which cover most practical applications. On the other hand the buoyancy parameter is varied from 0.033 to 0.2 while the height parameter ξ_b was taken to be 0.5, 0.75, and 1. It was found difficult to attain the correct value of f' at the axis at higher values of either ξ or ξ_b .

Buoyancy effects on the velocity and temperature distributions are depicted in figures (2-3) for $Pr=7$. From figure (2) it is clear that due to buoyancy effects an overshoot of the velocity has been occurred with the maximum velocity increasing from 1.14 to 1.25 as ξ increased from 0.4 to 0.8. Closer inspection of figure (2) reveals that the position of the maximum velocity gets closer to the axis as ξ increases. In contrast to the velocity profile, the temperature profile is less susceptible to buoyancy effects. This can be attributed to the fact that the direct effect of buoyancy is an additional force in the momentum equation.

As shown in figures (4-6) numerical solutions are obtained for the effect of the height parameter ξ_b on the velocity and temperature distributions where the buoyancy parameter is constant for all runs. The two figures show that the effect of increasing ξ_b is a decrease in both the velocity and temperature at the same axial position.

The effect of Prandtl number on both the velocity and temperature distributions is presented in figures (6-7). One sees that low Prandtl number fluids are more sensitive to buoyancy forces with the temperature profile more susceptible to Pr variation.

In figure (8) variations of the local Nusselt number $Nu/\sqrt{Re_x}$ with the buoyancy parameter ξ are presented for different values of the height parameter ξ_b , while such a relation is presented in figure (9) for different Prandtl numbers. As shown in figure (9) the value $Nu/\sqrt{Re_x}$ increases for higher Prandtl numbers while figure (8) shows that $Nu/\sqrt{Re_x}$ decreases as ξ_b increases.

Nusselt number based on the passage height $\Delta x_p = h_b b$ is derived to present Nusselt number versus the buoyancy parameter in the conventional manner. The effect of both the passage height Δx_p and Pr on Nusselt number defined as Nu_p is presented in figures (11-13). It is found that higher values of the height parameter Δx_p yield higher values of Nu_p and also higher values of Pr leads to higher values of Nusselt number.

Variation of the coefficient of skin friction C_f is presented in figure (13) as a function of the buoyancy parameter β over the range $0.033 \leq \beta \leq 1.2$ with a height parameter values of 0.5, 0.75 and 1. While the effect of Prandtl number on the coefficient of friction is presented in figure (12). The two figures show that lower values of either the passage height or Prandtl number yield higher values of the coefficient of friction. It is also clear that the Nusselt number and C_f trends are consistent with the expected effects of the aiding pressure gradient which accelerates the flow and increases both wall shear stress and heat transfer monotonically.

Comparison between the present work and that of M.G. Wasel [10] for laminar forced convection in the entrance region between two parallel plates reveals that the value of Nusselt number in case of mixed convection is about 40 percent higher than the corresponding value obtained in [10] as shown in figure (14).

5. CONCLUSIONS

The method of the local similarity solutions proved to be effective in the numerical analysis of combined forced and free convection flow between horizontal parallel plates. Numerical results for the coefficient of friction and local heat transfer are obtained for fluids having Pr numbers of .5, .7.1 and 2 and for values of the buoyancy parameter between 0.033-0.2. Local solutions at any axial position over this range could be obtained regardless of the upstream information. Efforts to extend the solution beyond 0.2 were unsuccessful in most runs. It is found that the coefficient of friction and heat transfer increase markedly as the buoyancy forces increase. Results obtained for the heat transfer are about 40 percent higher than those obtained by M.G. Wasel [10] for laminar forced convection between horizontal parallel plates.

REFERENCES

- [1] E.M. Sparrow and W.J. Minkowycz, buoyancy effects on boundary layer flow and heat transfer. Int. J. Heat. Mass Transfer, Vol 5 pp 505 1961.
- [2] D.G. Osborne and F.P. Incropera, laminar mixed convection heat transfer for flow between horizontal parallel plates with asymmetric heating, Int. J. Heat. Mass Transfer, vol. 28 NO . 1 PP 207 - 217 1985
- [3] W. Schneider, A Similarity solution for combined forced and free convection flow over a horizontal plate. J. Heat. Transfer, vol. 22 PP 1401 - 1406. 1970
- [4] K.J. Kennedy and A. Zebib, combined free and forced convection between horizontal parallel planes. Int. J. Heat Mass Transfer, vol 26 no. 3, PP. 471 - 474. 1983.
- [5] K.J. Kennedy and A. Zebib, combined forced and free convection between parallel plates. Paper 82-IH7048. Proc. 7th int. heat transfer conf. Hemisphere New York. 1982.

- [6] M. M. Abu-Zillal and S. M. Morcos, Buoyancy effects in the entrance region of horizontal rectangular channels, J. Heat Transfer Vol. 105 PP. 924-927 1983.
- [7] K. C. Cheng and G. J. Hwang, Numerical solution for combined free and forced laminar convection in horizontal rectangular channels, J. Heat Transfer pp. 59 - 66 Feb. 1969.
- [8] J. Wu, Ou, K. C. Cheng and R. C. Lin, combined free and forced laminar convection in inclined rectangular channels, Int. J. Heat Mass Transfer Vol. 19 PP. 277 - 282, 1976.
- [9] T. S. Chen, E. M. Sparrow, and A. Mucoglu, mixed convection in boundary layer flow on a horizontal plate J. Heat Transfer PP. 66 - 71 Fe. 1977.
- [10] M. G. Wasei, local similarity solution of laminar forced convection in the entrance region for flow between two parallel plates ,Mansoura Engineering J.Vol.14.No.1, June, 1989.

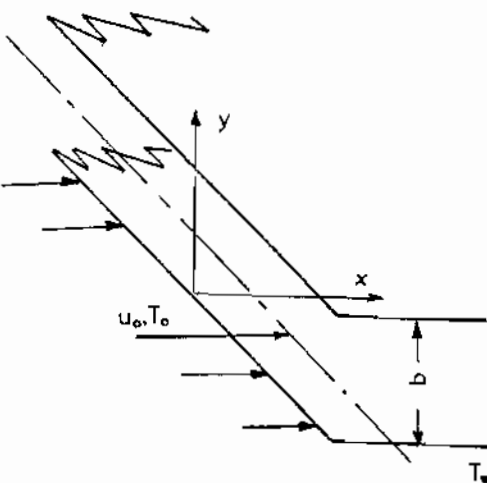
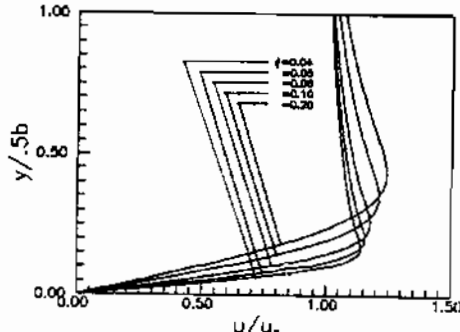


Fig.(1) configuration of the flow.

Fig.(2) effect of the buoyancy parameter ϵ on the velocity profile for $Pr=0.7, \beta_0=1$.

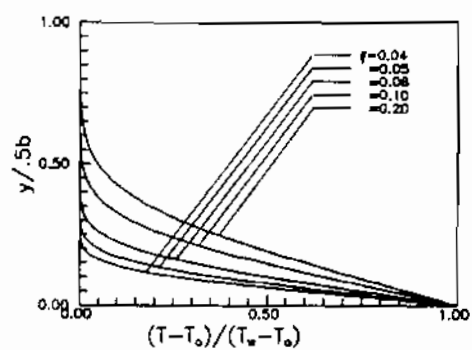


Fig.(3) effect of the buoyancy parameter f_1 on the temperature profile for $\text{Pr}=0.7$, $\xi_1=1.0$

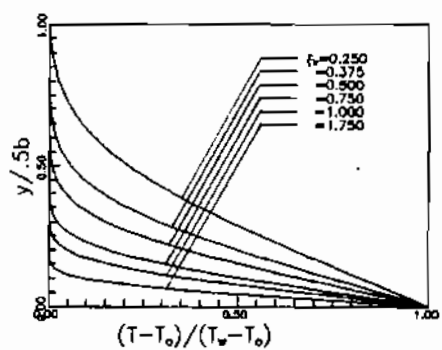


Fig.(4) effect of the height parameter f_2 on the temperature profile for $\text{Pr}=0.7$ and $\xi=1.0$

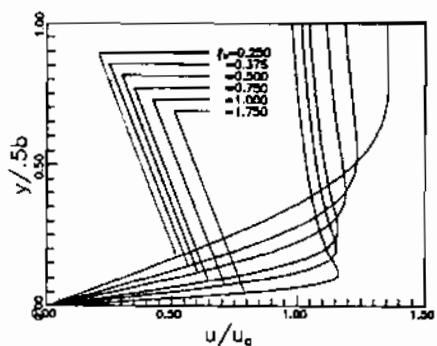


Fig.(5) effect of the height parameter ξ_1 on the velocity profile for $\text{Pr}=0.7$ and $f=0.5$

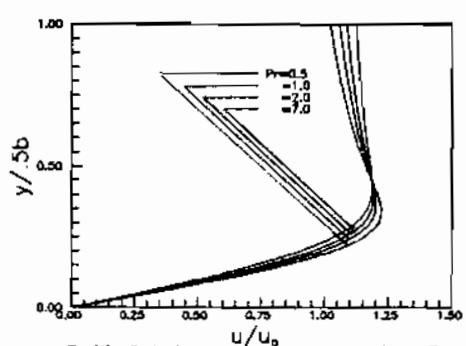


Fig. (6) effect of Prandtl number on the velocity profile for $f=0.1$, $\xi_1=1.0$

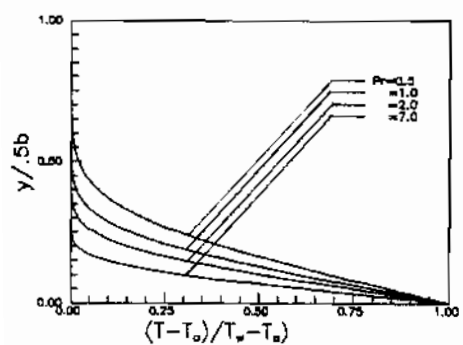


Fig. (7) effect of Prandtl number on the temperature profile for $f=0.1$, $\xi_1=1.0$

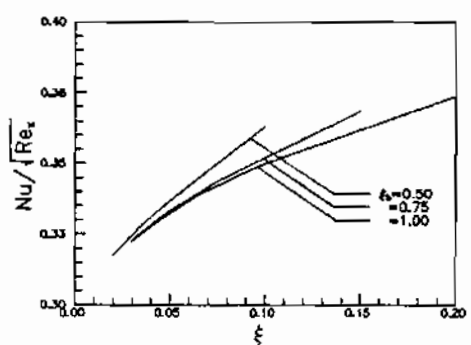


Fig.(8) effect of the height parameter f_2 on Nusselt number for $\text{Pr}=0.7$

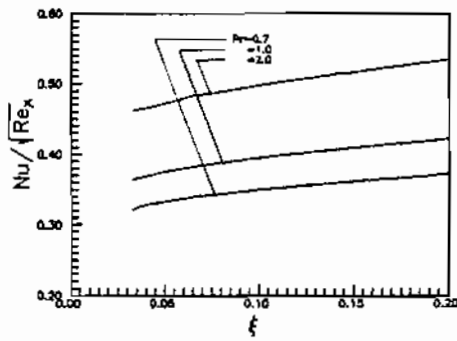
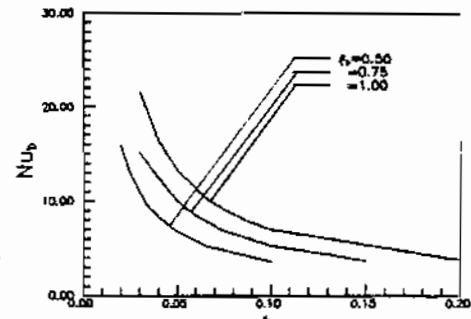
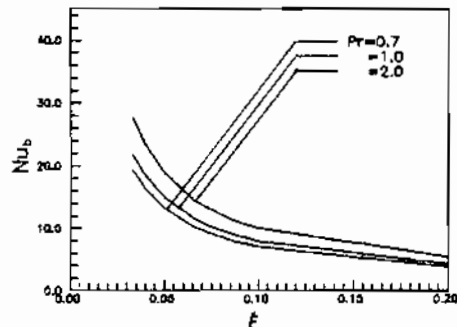
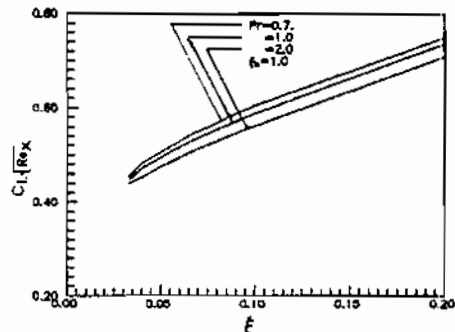
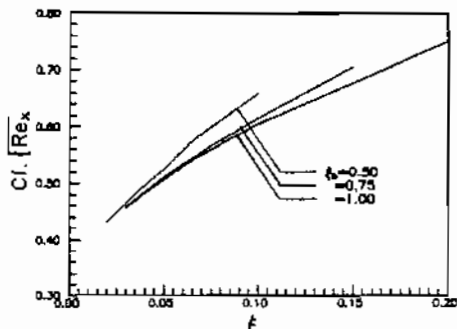
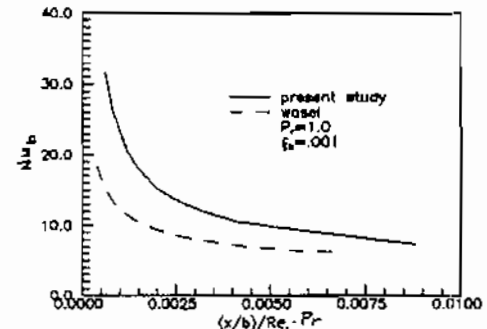
Fig.(9) effect of Prandtl number on the local heat transfer for $n_b=1.0$ Fig.(10) effect of the height parameter f_b on Nusselt number for $Pr=0.7$ Fig.(11) effect of Prandtl number on the local Nusselt number for $f_b=1.0$ Fig.(12) effect of Prandtl number on the coefficient of friction for $n_b=1.0$ Fig.(13) effect of the height parameter f_b on the coefficient of friction for $Pr=0.7$ 

Fig.(14) comparison between local Nusselt number of the present study with M.G. model 10 for forced convection.